Single-Step Preparation of TiO_2/MWCNT Nanohybrid Materials by Laser Pyrolysis and Application to Efficient Photovoltaic Energy Conversion

Jin Wang[1], Yaochen Lin[1], Mathieu Pinault[1], Arianna Filoramo[2], Marc Fabert[3], Bernard Ratier[3], Johann Bouclé[3*], Nathalie Herlin-Boime[1*]

[1]IRAMIS/NIMBE/LEDNA- LFP, CEA-CNRS URA 2453, CEA Saclay, 91191 Gif sur Yvette, France

[2]DSM/IRAMIS/NIMBE/LICSEN, CEA de Saclay, 91191 Gif sur Yvette, France

[3]XLIM UMR 7252, Université de Limoges/CNRS, 87060 Limoges Cedex, France

*Corresponding authors: johann.boucle@unilim.fr ; nathalie.herlin@cea.fr

1. Experimental details

1.1. Synthesis of TiO_2 and MWCNTs/TiO_2 nanocomposites by laser pyrolysis

The pure TiO_2 nanopowder and MWCNTs/TiO_2 *in situ* nanocomposite were synthesized by laser pyrolysis as previously described[1,2]. This method is based on the resonance of the emission of a CO_2 laser (10.6μm) with chemical precursors. Titanium tetraisopropoxide (TTIP, Sigma Aldrich, 97%) aerosol was first produced by an ultrasonic spraying technique (Pyrosol process). The produced droplets were then carried into the reactor chamber by an argon flow (2L/min), which plays also the role of confinement gas to avoid any interaction between the reactor walls and the precursors. In this work, 355 L/min of C_2H_4 was added in the precursor mixture (sensitizing gas) because of the poor absorption of the laser energy by TTIP.

Multi-wall carbon nanotubes (MWCNTs) were synthesized by aerosol-assisted catalytic chemical vapor deposition (CCVD). The synthesis set-up and standard procedures are presented in our previous works[3] Briefly,the precursor containing 1.25 wt% ferrocene in toluene was vaporized by an aerosol generator (Qualiflow-Jipelec Company, France) and carried into a reactor chamber by a mixed gas flow (0.7L/min Ar and 0.3 L/min H_2). The aerosol feeding rate is fixed at 0.57g/min, and the reaction temperature is maintained at 800°C. Following this procedure, the sample was formed of aligned CNT carpets covering the reactor walls.

Before using the synthesized MWCNTs, an annealing process at 2000°C during 2h under argon has to be applied to eliminate the iron atoms contained mainly in the nanotube central core[4]. Then, the annealed MWCNTs were dispersed during 2h in pure water containing 0.5wt% of MWCNTs and 1wt% of bile salt (sodium dodecyl sulfate, sodium deoxycholate and, Sigma-Aldrich) with an ultrasound probe (Bioblockvibracell 75043) working at 20 kHz and 375 W in pulse mode (1s on and 1s off)[5]. Well separated MWCNTs were obtained by filtrating this solution. The MWCNTs were then oxidized in a mixed solution of concentrated nitric-sulfuric acids (1:3) at 50°C for 2h, and filtered and washed. In the *in situ* case, the oxidized MWCNTs were re-dispersed in toluene and added into TTIP as the precursor for the synthesis by laser pyrolysis. These mixed precursors were introduced into the reactor chamber

and the synthesis was performed in a single step. In the *ex situ* case, the oxidized MWCNTs were re-dispersed in water and bile salt and then added into a TiO_2 paste, before a final 24-hours stirring step. In fact, toluene was also added into the precursor when we synthesized pure TiO_2 for *ex situ* composite to achieve similar dilution conditions than that of the *in situ* case.

All the as-formed NPs were annealed at 400°C for 3h to remove the free carbon phase that remains due to the decomposition of TTIP and/or C_2H_4.

1.2. Characterization techniques

Transmission Electronic Microscopy (TEM, Philips CM12) was used to observer the morphology of the nanocomposites. The Brunauer-Emmett-Teller (BET) method (Micromeritics FlowsorbII 2300) was applied to determine the specific surface of the nanopowders. The crystalline phases were measured by X-ray diffraction (XRD) with a Siemens D5000 instrument using the Cu-Kα radiation. The Fourier transform infrared spectra were obtained by the PERKING ELMER system 2000 FT-IR instrument. The quantity of oxygen atoms in MWCNTs was characterized by X-ray photoelectron spectra (XPS) (Kratos Analytical Axis Ultra DLD spectrometer, Al Kα X-ray) and elemental analysis instrument (Oxygen/Nitrogen/Hydrogen Analyzer EMA-800 series).

Raman spectroscopy was performed within the PLATINOM/OTPOLAS Platform at XLIM using a LabRAM HR Evolution spectrometer (Horiba).The apparatus is based on a microscope coupled to a 800mm focal length spectrograph. The excitation power is provided by a linearly polarized laser light at 633nm. After focusing through a x60 microscope objective, a spot of 6mW with a diameter of 2µm is available on the sample. The backscattered Raman light is collected by the microscope objective and directed towards the wide range spectrograph (220 - 2200nm, resolution min: 0.74 cm^{-1}). The analyses were performed on the powder under ambient conditions. After baseline removal, Raman maps were normalized to the most intense D band signature associated with MWCNT in the composites samples (MWCNT/TiO_2[*in situ*] sample containing 0.03wt% of CNT). Therefore, Raman maps are characteristics of the presence of MWCNT relatively to this sample.

Steady-state photoluminescence spectra were recorded using an FLS980 spectrometer (Edinburgh Instruments). The excitation was performed using a monochromated450W Xenon lamp and the detection was made in the 200-870nm range by a cooled R928P Hamamatsu photomultiplier (dark count <50cps). The sample were analyzed as powders using a quartz sample holder in a 45° geometry. Slit widths were adjusted to maximize the signal to noise ratio, leading to a spectral bandwidth of 1.5 nm approximately. All the spectra are normalized with regard to the emission pic at 3.15eV, which is attributed to the free exciton emission of anatase.

1.3. ssDSSCs fabrication and characterization

Device fabrication used the materials and methods previously reported[6,7]. The metal oxide pastes are prepared for pure TiO_2 and *in situ* MWCNTs/TiO_2 composite by dispersing the powders in an ethanol:α-terpineol mixture (weight ratio $M_{ethanol}$:$M_{\alpha\text{-terpineol}}$:$M_{TiO2}$= 5:4:1). Ethyl-cellulose (Aldrich) solution (10 wt.% in ethanol) is then added to obtain a TiO_2:EC weight ratio of 2:1.To obtain the *ex situ* MWCNTs/TiO_2 paste, a well dispersed oxidized MWCNTs solution were added into the pure TiO_2 paste. All these pastes were first stirred during 24h before using. The pastes were then deposited on Fluorine-doped tin oxide (FTO, 15Ω/□) coated glass substrates by spin-coating and the films were then progressively sintered up to 450°C during 40 minutes. In fact, these FTO substrates were previously coated by a TiO_2 compact layer deposited by chemical spray pyrolysis at 450°C.After a conventional $TiCl_4$ treatment for 2h, the porous electrodes were then immersed overnight in a diluted dye solution (0.3 mM, D102, Mitsubishi Paper Mills, Japan) dissolved in an tert-butanol: acetonitrile mixture (volume ratio of 1:1) at 80°C. The sensitized electrodes were then infiltrated by the spiro-OMeTAD solid-state hole conductor (Merck KGaA, Germany) by spin-coating. Finally, gold counter electrodes were evaporated under high vacuum on top of the device through a shadow mask that defines the active area (0.18 cm^2).

The morphology of the porous electrodes was observed by scanning electron microscopy (SEM, Carl Zeiss, Ultra 55). The photovoltaic performance measurements of the devices were recorded using a Keithley 2400 source-measure unit in the dark and under simulated solar emission (Atlas Solarconstant 575PV) at 1 sun after spectral mismatch correction. A certified calibration silicon cell (NEWPORT) was used as reference photodiode. The incident photon-to-current efficiency (IPCE) was obtained by a monochromated 75W Xenon lamp (Newport) and a calibrated pico-amperemeter. Transient photovoltage decay measurements were performed on ssDSSCs under open-circuit conditions. The incident white illumination was provided by 2 OSRAM LEDs, leading to a power density up to 80 mW cm^{-2} on the active area of the cells. A third green LED (λ=550nm, Luxeon STAR, 5W) was used to generate the additional light pulse and the transient signals were recorded using a digital oscilloscope (Tektronics DPO4032).

It is worth noting that several sets of independent devices were prepared and characterized. They all exhibit the same trends. In this work, the reported photovoltaic performance is associated with a representative set of devices which was randomly chosen.

2. Results and discussion

The estimated mean crystal diameters of *in situ* and *ex situ* composite are presented inTable S1, as well as the Brunauer-Emmett-Teller (BET) specific surface area and diameters.

Table S1 - BET, TEM and XRD mean crystal diameters of the powders synthesized by laser pyrolysis

	BET	XRD	TEM

	Specific surface (m^2/g)	Diameter (nm)	Mean crystal diameter (nm)	Mean grain diameter (nm)
TiO_2	122	12	10	11.7
MWCNT/TiO_2[*in situ*]	116	13	11	11.8
MWCNT/TiO_2[*ex situ*] 0.03 wt%	120	12	10	11.7

The samples exhibit similar particle sizes, with estimated BET diameters slightly larger than crystallite diameters that usually indicate the presence of amorphous regions in the powders. From TEM images (Figure S5), a similar size was measured for TiO_2 nanoparticles in all samples (counting 100 nanoparticles) and a "chain-like" morphology is noted at larger scale. This specific feature was suggested to improve the infiltration of the solid-state hole transporter (spiro-OMeTAD) into the porous TiO_2 electrode of devices made from laser pyrolysis particles.[5] The good agreement between the different methods used for diameter measurement indicates that very low amount of MWCNT does not significantly modify the BET surface. Very comparable morphologies are found for all the samples used for this study.
The Fourier transform infrared spectroscopy (FTIR) spectra (Figure S1) reveal the appearance of functional groups, such as –COOH, on the surface of the MWCNTs. The XPS spectra (Figure S2) confirm also this trend. The oxygen content increases from 1 to 5at% for non-oxidized and oxidized nanotubes respectively. Such chemical groups are expected to favor the grafting of TiO_2 particles on the surface of MWCNTs[8] The mean length of the MWCNTs is found to be around 0.9µm. Most of tubes are found to be below 2 µm long ($\emptyset \approx 25nm$) (Figure S3,). This mean length was measured before being introduced into TTIP.

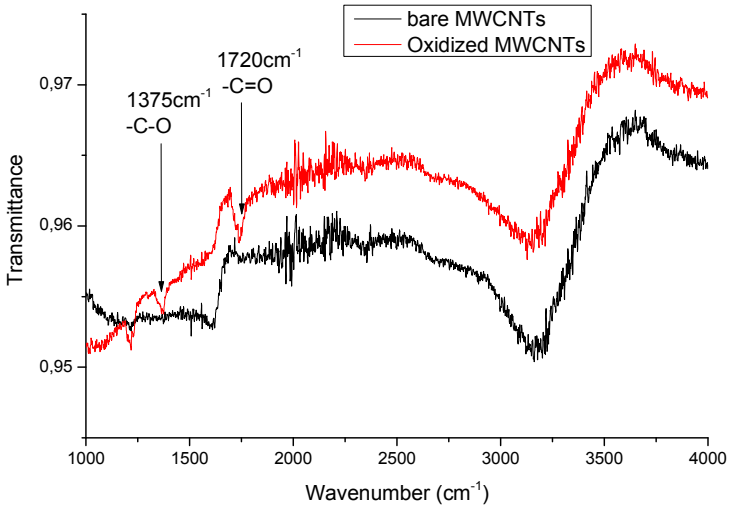

Figure S1 - Fourier transform infrared spectra of bare MWCNTs and Oxidized MWCNTs

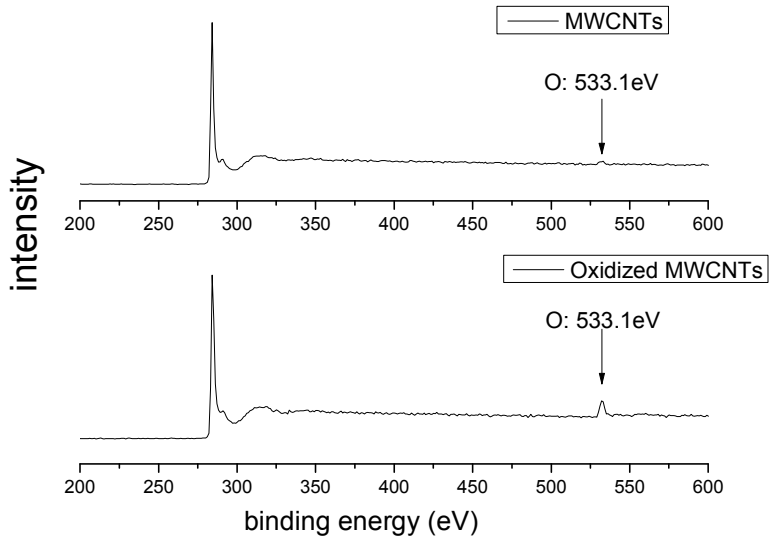

Figure S2 - XPS spectra of pure MWCNTs and oxidized MWCNTs

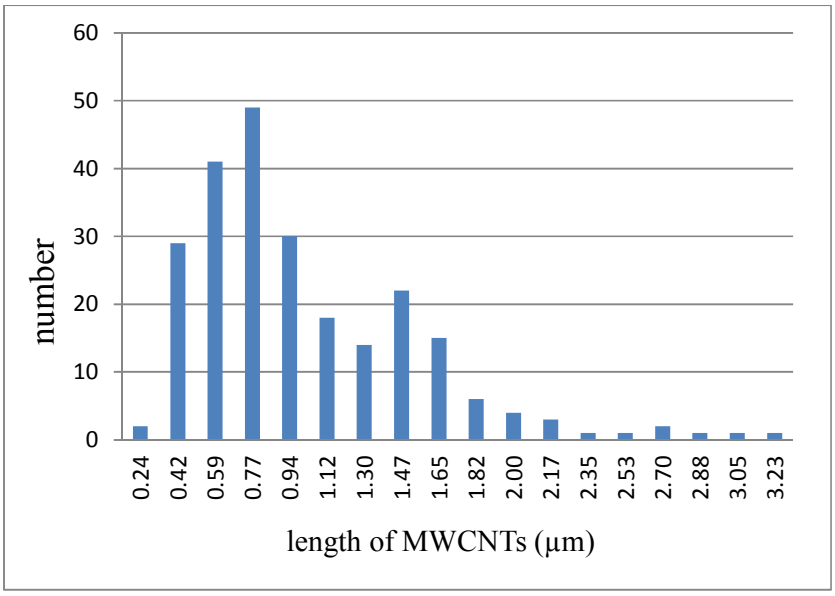

Figure S3 - Length distribution of dispersed MWCNTs

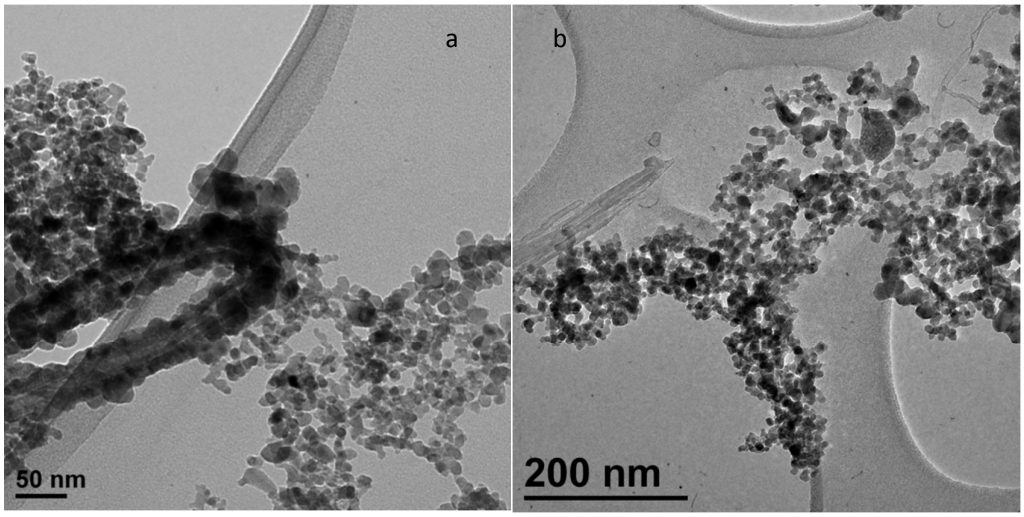

Figure S4 - TEM images of the two nanopowders synthesized in this study: (a) MWCNT/TiO_2 [*in situ*] (b) reference TiO_2

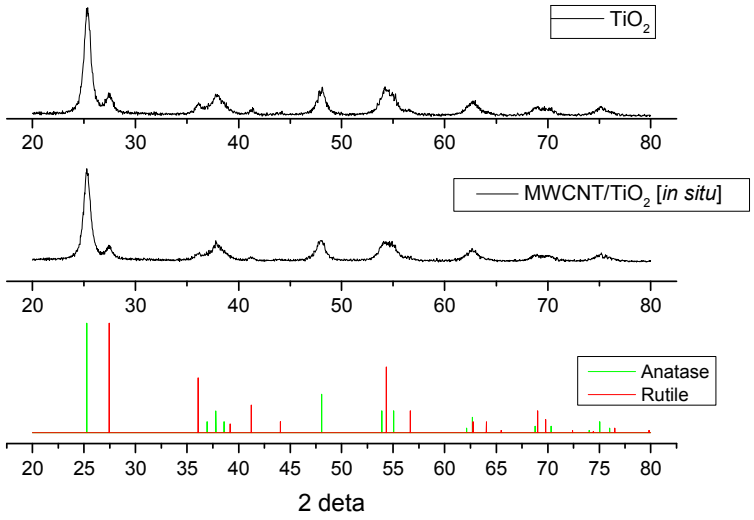

Figure S5- XRD patterns of pure TiO_2 and MWCNT/TiO_2[*in situ*] nanocomposite containing 0.03wt% of CNT.

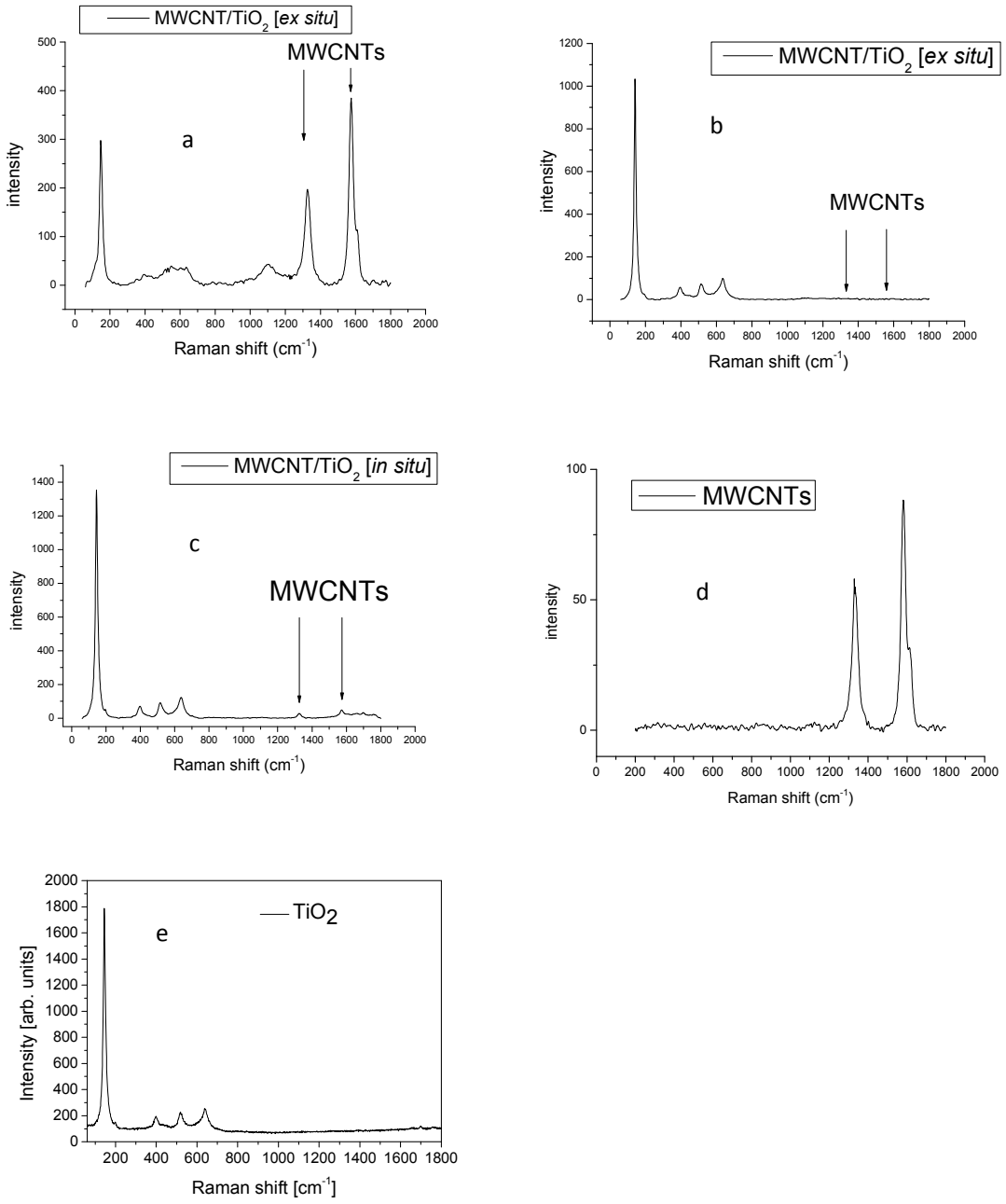

Figure S6- Raman spectra of (a,b): MWCNT/TiO_2 [*ex situ*]containing 0.1wt%CNTs (c): MWCNT/TiO_2 [*in situ*] containing 0.03wt% CNTs (d) MWCNTs .(e) pure TiO_2

Figure S6a was recorded at a particular spot where a high amount of MWCNTs was observed. The Raman spectra at the greenest point of the analysis zone of Figure 2a for MWCNT/TiO_2 [*ex situ*] is presented in Figure S6b. This great difference in intensity of the MWCNTs signal indicates that this *ex situ* composite is highly heterogeneous. As for the MWCNT/TiO_2 [*in situ*] composite, the greenest point of Figure 2b is presented in Figure S6c. The *in situ* composite is found to be much more homogeneous.

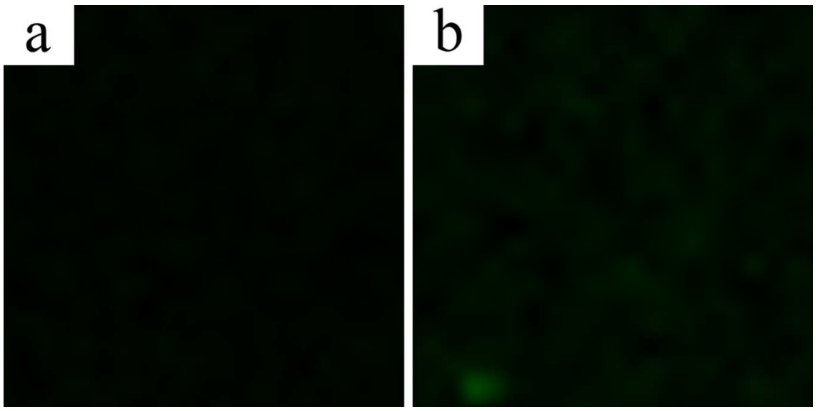

Figure S7- Raman maps over 40×40 square micrometers associated to the disorder mode (D band) of MWCNTs within (a) pure TiO_2 and (b) MWCNT/TiO_2 [*ex situ*] composites containing 0.03wt% CNTs.

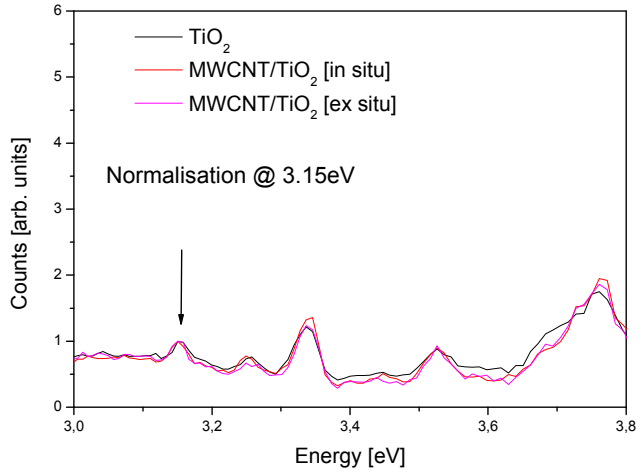

Figure S8- Photoluminescence (PL) spectra of TiO_2, MWCNT/TiO_2 [*ex situ*] and MWCNT/TiO_2 [*in situ*](0.03wt% CNTs) powder in the region corresponding to the free exciton emission of anatase (3-3.8eV)

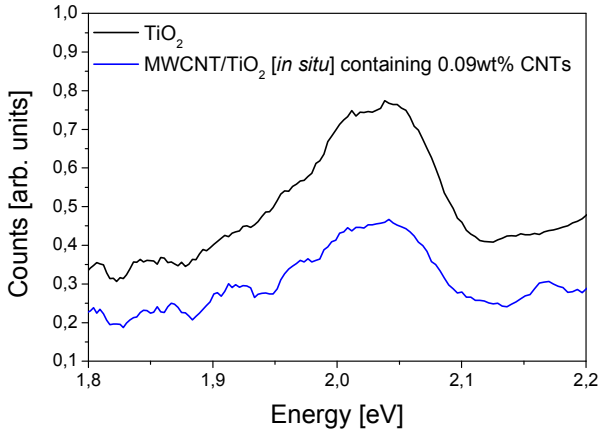

Figure S9 - Photoluminescence (PL) spectra of pure TiO_2 and MWCNTs/TiO_2[*in situ*] containing 0.09wt% of CNTs

Table S2 - Photovoltaic performance of the ssDSSCs based on *ex situ* nano composite with different MWCNTs doping amount.

CNT content in the *ex situ composite*	V_{oc}(V)	J_{sc} (mA/cm^2)	FF	η(%)
-	0.78	6.93	0.70	3.78
0.01%	0.79	6.71	0.70	3.69
0.03%	0.78	6.92	0.70	3.74
0.06%	0.80	5.87	0.72	3.37
0.1%	0.77	5.62	0.73	3.19
0.5%	0.76	6.07	0.57	2.61
1%	0.77	4.60	0.47	1.68
2%	0.76	3.96	0.53	1.61

Table S2summarizes the photovoltaic parameters under 1 sun of the ssDSSCs based on the *ex situ* nanocomposite with different MWCNTs doping amounts. This set of cells is independent than that discussed on the core of the article, leading to slight variation of the parameters. The trends discussed in the paper are global trends that have been observed and confirmed several times. Thesolar cell efficienciescorresponding to low MWCNTs contents (below 0.03wt%) arequitecomparable to that of the reference device (pure TiO_2). Above 0.06wt% of CNT, the efficiency decreasesdrastically with the MWCNTs content.

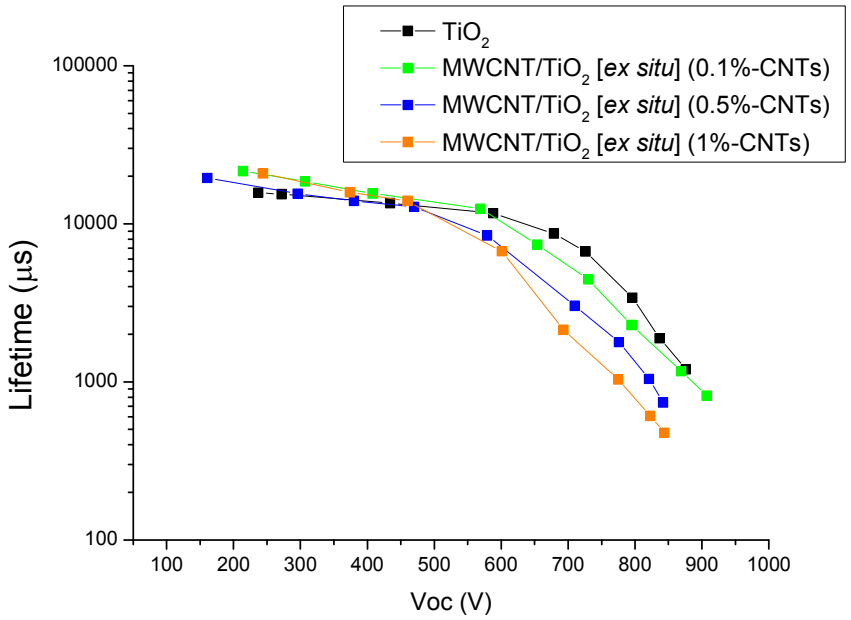

Figure S10- Electron lifetimes in ssDSSCs with pure TiO_2 and$MWCNT/TiO_2$ [*ex situ*] containg 0.1%, 0.5% and 1% CNTs

Table S3- Photovoltaic performance of ssDSSCs based on *in situ* composites with different MWCNTs doping amounts.

CNT content in the *in situ composite*	V_{oc}(V)	J_{sc} (mA/cm^2)	FF	η(%)
-	0.77	6.52	0.68	3.41
0.03%	0.76	7.78	0.70	4.13
0.09%	0.78	7.19	0.64	3.66

Table S3summarizes the photovoltaic parameters under 1 sun of ssDSSCs based on *in situ* nanocomposites with different MWCNTs doping amounts. This set of cells is independent of the one discussed on the core of the article, leading to slight variation of the parameters. The trends discussed in the paper are global trends that have been observed and confirmed several times.

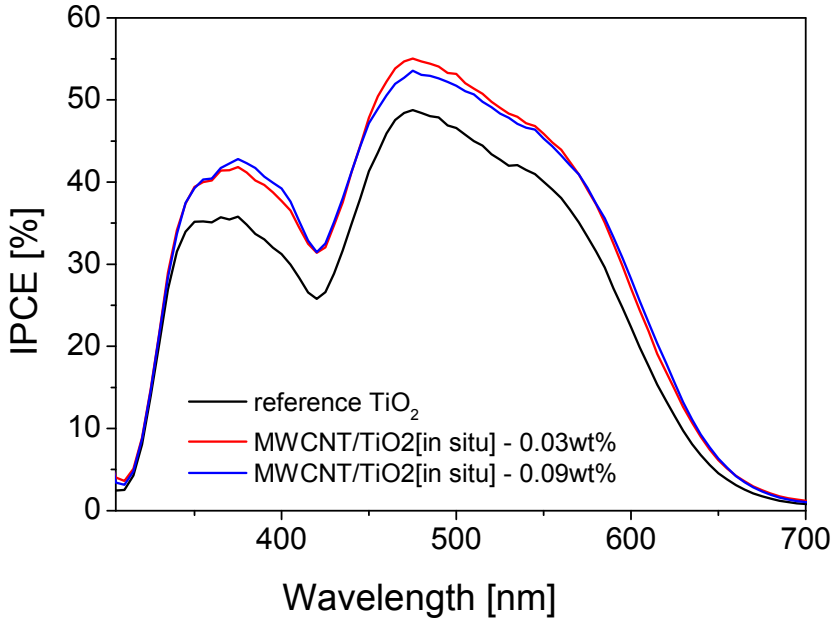

Figure S11–IPCE spectra of ssDSSCs with pure TiO_2 and MWCNT/TiO_2 [*in situ*] for two different CNT contents: 0.03wt% and 0.09wt%. The data associated with a cell based on pure TiO_2 is presented for reference.

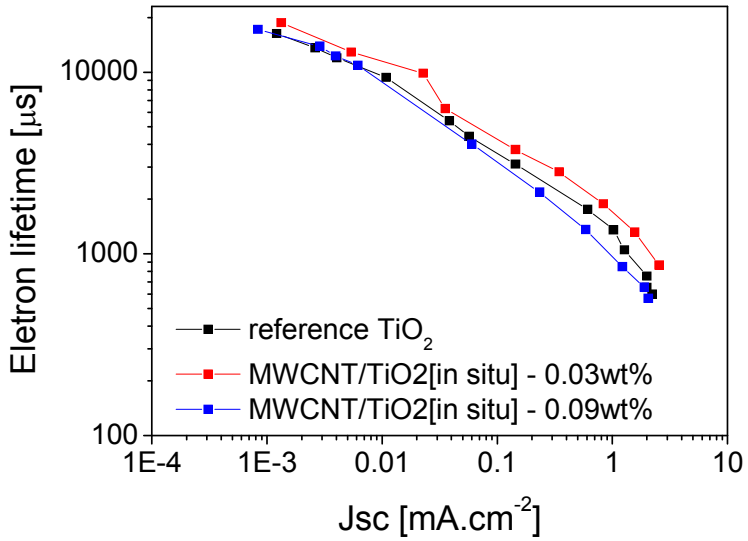

Figure S12- Electron lifetimes measured by transient photovoltage for ssDSSCs with pure TiO_2 and MWCNT/TiO_2 [*in situ*] for two different CNT contents: 0.03wt% and 0.09wt%. The data associated with a cell based on pure TiO_2 is presented for reference.

References

(1) Simon, P.; Pignon, B.; Miao, B.; Coste-Leconte, S.; Leconte, Y.; Marguet, S.; Jegou, P.; Bouchet-Fabre, B.; Reynaud, C.; Herlin-Boime, N. N-Doped Titanium Monoxide Nanoparticles with TiO Rock-Salt Structure, Low Energy Band Gap, and Visible Light Activity. *Chem. Mater.* **2010**, *22*, 3704–3711.

(2) Pignon, B.; Maskrot, H.; Guyot Ferreol, V.; Leconte, Y.; Coste, S.; Gervais, M.; Pouget, T.; Reynaud, C.; Tranchant, J.-F.; Herlin-Boime, N. Versatility of Laser Pyrolysis Applied to the Synthesis of TiO2 Nanoparticles – Application to UV Attenuation. *Eur. J. Inorg. Chem.* **2008**, *2008*, 883–889.

(3) Castro, C.; Pinault, M.; Porterat, D.; Reynaud, C.; Mayne-L'Hermite, M. The Role of Hydrogen in the Aerosol-Assisted Chemical Vapor Deposition Process in Producing Thin and Densely Packed Vertically Aligned Carbon Nanotubes. *Carbon* **2013**, *61*, 585–594.

(4) Pinault, M.; Mayne-L'Hermite, M,; Reynaud, C.; Beyssac, O.; Rouzaud, J.N.; Clinard, C. Carbon Nanotubes Produced by Aerosol Pyrolysis: Growth Mechanisms and Post-Annealing Effects, *Diamond Relat. Mater.* **2004**, 13, 1266–1269

(5) Glory, J; Mierczynska, A.; Pinault, M.; Mayne-L'Hermite, M.; Reynaud, C.; Dispersion Study of Long and Aligned Multiwalled Carbon Nanotubes in Water, *J. Nanosci. Nanotechnol.* **2007**, *7*, 1-5.

(6) Melhem, H.; Simon, P.; Wang, J.; Di Bin, C.; Ratier, B.; Leconte, Y.; Herlin-Boime, N.; Makowska-Janusik, M.; Kassiba, A.; Bouclé, J. Direct Photocurrent Generation from Nitrogen Doped TiO_2 Electrodes in Solid-State Dye-Sensitized Solar Cells: Towards Optically-Active Metal Oxides for Photovoltaic Applications. *Sol. Energy Mater. Sol. Cells* **2013**, *117*, 624–631.

(7) Melhem, H.; Simon, P.; Beouch, L.; Goubard, F.; Boucharef, M.; Di Bin, C.; Leconte, Y.; Ratier, B.; Herlin-Boime, N.; Bouclé, J. TiO_2 Nanocrystals Synthesized by Laser Pyrolysis for the Up-Scaling of Efficient Solid-State Dye-Sensitized Solar Cells. *Adv. Energy Mater.* **2011**, *1*, 908–916.

(8) Yu, J.; Fan, J.; Cheng, B. Dye-Sensitized Solar Cells Based on Anatase TiO_2 Hollow Spheres/Carbon Nanotube Composite Films. *J. Power Sources* **2011**, *196*, 7891–7898.

This information is available free of charge via the Internet at http://pubs.acs.org/.